J. Phys. B: At. Mol. Opt. Phys. **25** (1992) 1607–1620. Printed in the UK

Crossed-beam experiment for the scattering of low energy electrons from CF_4*

L Boesten†, H Tanaka†, A Kobayashi†§, M A Dillon‡ and M Kimura‡

† Department of General Science and Physics, Sophia University, Chiyoda-ku, Tokyo 102, Japan

‡ Argonne National Laboratory, 9700 S Cass Avenue, Argonne, IL 60439, USA

Received 4 September 1991, in final form 10 December 1991

Abstract. Differential scattering cross sections (DCS) for electron–CF_4 collisions in the energy range from 1.5 to 100 eV were measured with a crossed beam instrument for scattering angles of 15° to 130°. The DCS are normalized by reference to He. Integral and momentum transfer cross sections are compared with measurements of total cross sections, swarm experiments and theory. The integrated DCS show a broad structure at 7 eV of symmetry T_2 as predicted by theory, and one broad peak from 15 to 25 eV. The observed peaks differ in magnitude and angular distribution from recent SMC calculations. Evidence of a shape resonance of T_2 symmetry was observed in the recorded angular distributions for vibrational modes ν_0, ν_1, ν_3, and ν_4. In addition a large cross section for ν_3 excitation with 2 eV electrons was found to occur by a direct mechanism.

1. Introduction

CF_4 is one of the more commonly used etchant gases for dry-etching and has a large mean electronic energy (>7–15 eV, Christophorou 1984). Beyond 12 eV, large dissociation cross sections set in (Winters *et al* 1982) while at energies below 10 eV negative ions and neutral radicals are formed by dissociative electron attachment (Harland and Franklin 1974, Scheunemann *et al* 1982, Spyrou *et al* 1983, Lotter *et al* 1989).

Past investigations of the low energy electron scattering have concentrated on measurements of the total cross sections (Verhaart *et al* 1978, Jones 1986, Curtis and Walker 1989), on momentum transfer (Kurachi and Nakamura 1990), ionization (Leiter *et al* 1984), attachment cross sections (MacNeil and Thynne 1970, Naidu and Prasad 1972, Chutjian 1981) and swarm parameters (Curtis *et al* 1988). Oscillator strengths were obtained from zero-angle electron energy loss spectra by Harshbarger and Lassettre (1973) and King and McConkey (1978) at impact energies of 400–500 eV. The only measurement of vibrationally elastic scattering by a crossed beam method is that of Sakae *et al* (1989) for impact energies above 75 eV. No DCS have been reported for the low energy region <50 eV so crucial for plasma operation.

* Work supported by the US Department of Energy, Office of Energy Research, Office of Health and Environmental Research, under contract W-31-109-Eng-38, and by a Grant in Aid from the Ministry of Education, Science, and Culture, Japan.

§ Present address: Nichiden Anelva Co., Fuchuu, Yotsuya 5-8-1, Tokyo, Japan.

0953-4075/92/071607+14$04.50

There are only two theoretical investigations. CF_4 was calculated among other gases as a test case for the continuum $X\alpha$ multiple scattering method (CMS) by Tossel and Davenport (1984), and more recently by Huo (1988) in a multichannel extension of the Schwinger variational principle (SMC).

In this paper, we present absolute differential cross sections for vibrationally elastic and inelastic scattering of CF_4 in the energy range from 1.5 to 100 eV over an angular range from 15° to 130°. The elastic DCS were extrapolated to 0 and 180° by phase shift fitting and numerically integrated. The resulting integrated and momentum transfer cross sections σ_I and σ_M are compared with available measurements of the total cross section and other swarm experimental data. Two (three?) broad humps in σ_1 and in the angular distributions are readily interpreted in terms of a shape resonance of symmetry T_2 in accordance with the SMC calculation. The T_2 symmetry is confirmed by a symmetry analysis of the vibrational enhancement.

2. Experiment

The spectrometer and experimental procedures have been previously described in detail (Tanaka *et al* 1988, 1990a). Energy-selected electrons from a hemispherical monochromator are focused onto a molecular beam. Electrons scattered into a small solid angle are energy analysed by a differentially pumped hemispherical analyser and recorded. Absolute differential cross sections for both elastic and inelastic scattering are obtained by normalizing to a set of recommended elastic He DCS (Boesten and Tanaka 1991a). The incident electron energy was calibrated against the 19.37 eV resonance of He. The four fundamental vibrational modes of CF_4 have energies $\nu_1 = 113$, $\nu_2 = 54$, $\nu_3 = 159$, and $\nu_4 = 78$ meV. With the present resolution of 35–40 meV, the elastic peak is clearly separated, but ν_2 and ν_4 overlap to some extent. Rotational structures are not resolved. Experimental errors are estimated as 15–20% for elastic DCS and 30% for vibrational excitation.

3. Experimental results

3.1. Elastic scattering

Vibrationally elastic DCS were measured at the energies shown in table 1 from 1.5 to 100 eV and for scattering angles from 15° to 130°. Figure 1 repeats the same data in the form of a three-dimensional plot. At 100 eV, our data agree with those of Sakae *et al* (1989) to within 10% over 15° to 90°, but our minimum (at 100°) is deeper and the tail raises less steeply to only 70% of their value at 130°, cf figure 2. In the same figure we also compare a few selected angular distributions with those of CH_4 (Boesten and Tanaka 1991b). Below 10 eV, CF_4 lacks the deep high-angle minimum, and the broad peak shifts to lower angles with decreasing impact energy. Above 15 eV, the DCS of CF_4 undulate more frequently and are larger. The present experimental comparison differs considerably from a previous purely theoretical comparison (Huo 1988). Figure 2 also contains a plot of Huo's theory which she based on a Schwinger variational principle extended to polyatomic molecules and applied at a fixed nuclei static-exchange level. Her calculations approximately reproduce the experiments at 10, 15, 20 and 35 eV for forward scattering, but miss the broad maximum at 90°, 10–20 eV.

Table 1. DCS of CF_4 in units of 10^{-16} cm^2 sr^{-1} and 10^{-16} cm^2.

θ (deg)	1.5 eV	2 eV	3 eV	5 eV	6 eV	7 eV	8 eV	9 eV	10 eV	15 eV	20 eV	35 eV	50 eV	60 eV	100 eV
15	—	0.1189	0.3408	0.9647	1.5526	2.5565	3.7041	4.7153	4.4007	5.4326	6.7566	14.1044	13.3217	12.1904	9.9255
20	0.1156	0.2107	0.5437	1.1780	1.6739	2.4716	3.5055	4.0973	4.7677	4.8219	5.1461	7.8265	6.9383	5.8892	3.4611
30	0.2929	0.5174	0.9571	1.7782	2.0409	2.3776	2.9866	3.5126	4.1163	3.4725	3.1666	2.6912	1.4085	1.0154	1.0555
40	0.4755	0.7532	1.2560	2.1309	2.3629	2.4221	2.4890	2.6564	2.8836	2.4642	1.7198	0.8776	0.7378	0.7464	0.7534
50	0.8106	1.1179	1.5905	2.3340	2.4184	2.0523	1.7570	1.7135	1.6848	1.3828	0.9118	0.8609	0.8566	0.7594	0.3187
60	0.9146	1.3994	1.6028	2.0814	1.9375	1.7795	1.1971	1.1146	0.9990	0.9010	0.7949	0.9268	0.6723	0.4286	0.2172
70	1.0264	1.2575	1.5126	1.4717	1.4839	1.1095	0.7749	0.7199	0.7302	0.8689	1.0042	0.8090	0.3603	0.2190	0.2153
80	0.9225	1.0442	1.1786	1.0226	0.9028	0.6573	0.5520	0.6045	0.7817	1.0580	1.0952	0.4353	0.1696	0.1289	0.1571
90	0.8779	0.8065	0.8906	0.6066	0.5430	0.4349	0.4953	0.6814	0.7996	1.0762	0.9876	0.2011	0.1364	0.1275	0.0995
100	0.8154	0.7264	0.5381	0.4080	0.3774	0.4683	0.5924	0.7671	0.7938	0.9311	0.6900	0.1760	0.1331	0.1237	0.0948
110	0.6146	0.4861	0.4399	0.3552	0.4347	0.5385	0.6781	0.7541	0.7272	0.6981	0.5303	0.2550	0.2002	0.1851	0.1223
120	0.4576	0.4031	0.3167	0.3363	0.4473	0.5927	0.6703	0.7307	0.6215	0.5948	0.5540	0.4546	0.4086	0.3220	0.1917
130	0.3618	0.2978	0.2637	0.3782	0.4503	0.5735	0.6118	0.6584	0.6514	0.6907	0.8226	0.6906	0.6573	0.4328	0.2619
σ_I	7.738	8.555	10.46	12.72	13.40	13.36	13.91	15.40	16.63	16.92	17.63	16.72	14.24	13.06	9.844
σ_M	6.963	7.136	7.645	8.243	8.620	8.781	9.124	10.24	11.38	13.49	14.11	8.757	6.722	5.836	3.848

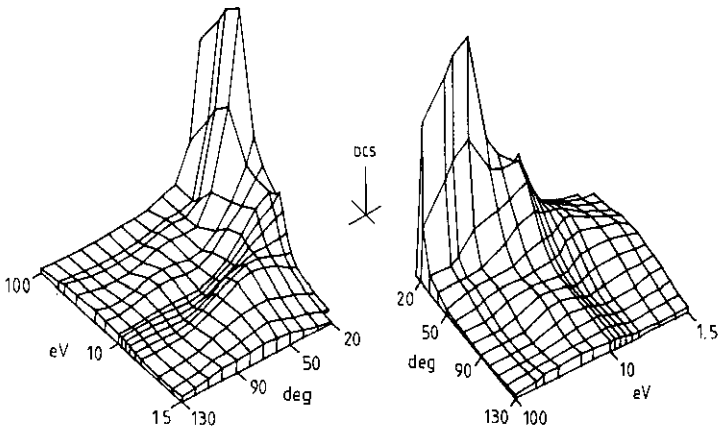

Figure 1. Observed elastic DCS. Energy markings correspond to the entries of table 1.

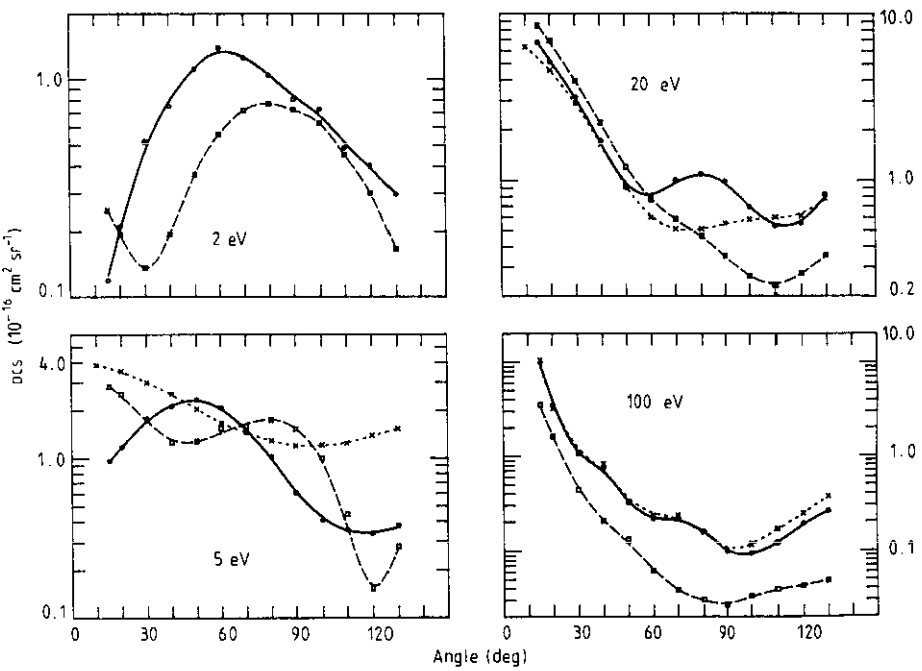

Figure 2. Comparison of observed elastic DCS of CF_4 (——) with those of CH_4 (— —). Calculations of Huo (1988) at 5 eV and 20 eV (—×—), and measurements of Sakae *et al* (1989) at 100 eV (—×—) are included.

The differences become more pronounced at lower impact energies. At 25 to 35 eV, the shape of her DCS resembles our data, but magnitudes differ.

3.2. Fitting and integration

In figure 3 we present the elastic integral and momentum cross sections. These were determined by modified phaseshift fitting for 1.5 to 10 eV and by inelastic phaseshift fitting for 10-100 eV as described recently (Boesten and Tanaka 1991b). We assume

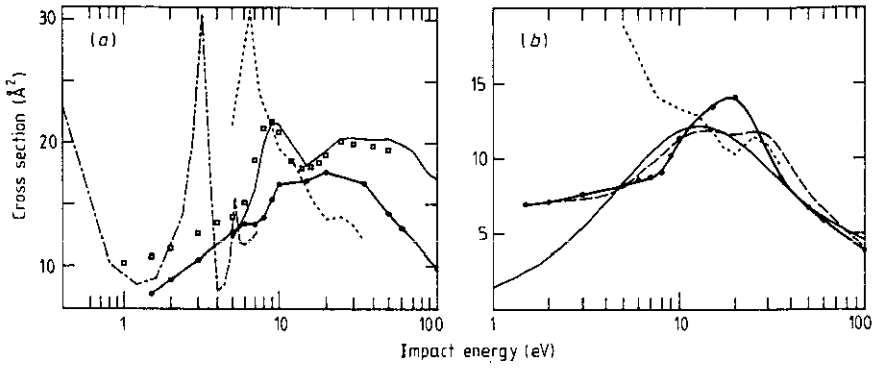

Figure 3. (*a*) Integral cross sections (Q_i, thick full curve) together with measured total cross sections of Jones (1986, Q_T, □), Nishimura (1991, Q_T, ——), the theoretical cross sections of Tossel and Davenport (1984, Q_T, — · —, scaled down to $\frac{1}{3}$ of his values) and those of Huo (1988, Q_i, – – –). (*b*) Momentum transfer cross section (Q_M, thick full curve) together with the measurement of Kurachi and Nakamura (1990, — —), the estimate of Hayashi (1991, ——) and the calculation of Huo (1988, – – –).

that for integration purposes elastic scattering by a tetrahedral molecule, averaged over all molecular directions, can be approximated by a central field formula.

$$d\sigma/d\omega = |f(\theta)|^2 \tag{1}$$

$$2ikf(\theta) = N_k\left\{\sum_{l=0}^{L}[S_l(k)-1](2l+1)P_l(\cos\theta)+CL(\theta)\right\} \tag{2}$$

$$CL(\theta) = 2ip\alpha k^2\left[\tfrac{1}{3}-\tfrac{1}{2}\sin(\theta/2)-\sum_{l=1}^{L}P_l(\cos\theta)/\{(2l+3)(2l-1)\}\right] \tag{3}$$

Here $CL(\theta)$ is the Born approximation of the higher phaseshifts δ_l, k is the wavenumber, α the molecular polarizability, P_l are the Legendre polynomials and f is the scattering amplitude. $S_l(k) = \exp\{2i\delta_l\}$ for modified, and $S_l(k) = \eta_l \exp\{2i\delta_l\}$ for inelastic phase-shift fitting with inelasticity parameter η_l. N_k (size 0.75–1.5) is an overall fitting parameter used now for elastic and inelastic fitting. With only twelve measurements per range (15° data discarded) the fits are sensitive to noise but repetition of measurements and fits reproduced the integrals to within 10%–15%. The selection of fits follows the criteria given in the above paper. Figure 3 includes some total cross sections found in the literature, and the two calculations mentioned above.

Energy losses of CF_4 can be divided into two regions, one below 12.7 eV where—in the present context—only vibrational excitation takes place, and another above 12.7 eV which is the regime of electronic excitation. The integrated elastic cross sections σ_1 show a shoulder at about 7 eV where a peak of dissociative attachment is known to exist (cf Lotter *et al* and other sources cited in the introduction), and a broad hump at 15–25 eV. The 'feature' at 10 eV arises mainly from low angle contributions and is discussed in Huo (1988). Because of the peculiar nature of the inelastic excitations in the whole range (Hayashi 1987), the shape of the cross sections diverges considerably from that of CH_4. The Ramsauer-Townsend minimum at 0.16 eV (Field *et al* 1984) almost coincides with the excitation energy of mode ν_3. The peaks of the MS Xα calculation are way off in size and position while those of Huo approach our results in location, but not in size.

We have subtracted our σ_I point by point along the energy scale from the total cross sections Q_T of Jones/Nishimura thus extracting the sum of inelastic DCS, and compare these in figure 4 with the sum of inelastic cross sections from swarm experiments (Kurachi and Nakamura 1990). The agreement in shape and position is good if one remembers that differences are sensitive to errors (>15% in σ_I) and that unfolding of swarm experiments probably smooths out local features.

3.3. Vibrational excitation

Electron-CF_4 collisions at low electron energies are characterized by a mixture of direct and resonance-enhanced scattering. Figure 5 shows the energy dependence of the cross section of the totally antisymmetric mode ν_3 at 90°. This is the intense mode in the energy range under study. The scattering is dominated by three features, a steep ascent for energies approaching the vibrational excitation threshold, a strong enhancement in the form of a broad peak at 8 eV, and a weak and very broad resonance at

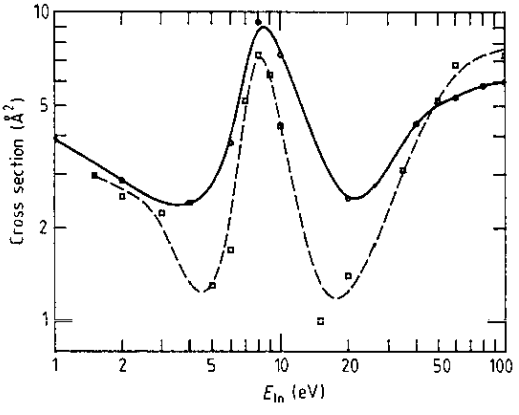

Figure 4. Inelastic cross sections. Point by point difference (– – –) between Q_T (Jones 1986/Nishimura 1991) and our σ_I: sum of inelastic DCS from swarm experiments (Kurachi and Nakamura 1990, ——).

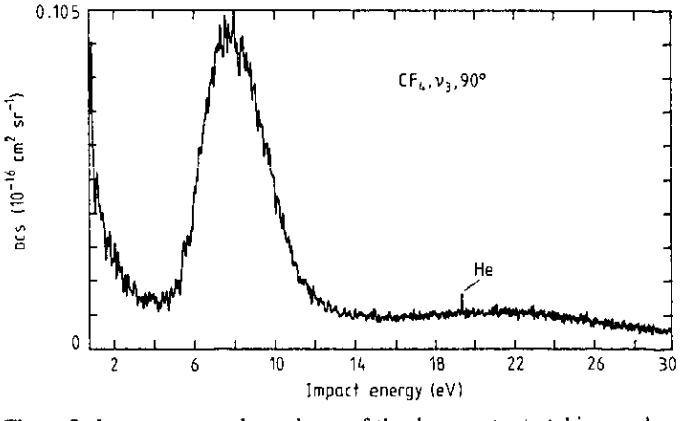

Figure 5. Impact energy dependence of the degenerate stretching mode ν_3 ($\Delta E = 0.16$ eV) for a scattering angle of 90°. The horizontal scale starts at 0.8 eV. The small peak at 19 eV arises from the use of non-resonant He DCS in the normalization step.

21 eV. Typical energy-loss spectra for the vibrational excitation at 2 and 8 eV are compared in figure 6.

CF_4 is one of the few gases where modes ν_1 and ν_3 can be observed separately. At low angles ν_3 becomes much stronger than the elastic DCS which decreases towards the Ramsauer-Townsend minimum, cf figure 6. A similar effect has been observed in SF_6 (Rohr 1977). Figure 7 shows an example of the decomposition of the 8 eV energy loss spectrum into the single vibrational modes and harmonics up to $2\nu_3$. Assumed were possible peaks at positions ν_4, ν_1, ν_3, $2\nu_1$, $\nu_1+\nu_3$, $2\nu_3$ (and $3\nu_3$, not shown). Note especially that correct reproduction of the first inelastic peak requires ν_1. Inclusion of ν_2 (at about $0.7\nu_4$) produces small negative sizes at nearly all angles from which we conclude that it either is not present or cannot be distinguished from the apparatus function. Both ν_1 and ν_2 are optically forbidden. At 20 eV decomposition of the weak signal becomes ambiguous: If ν_2 is included, ν_2 has a minimum at 50° while ν_4 fluctuates wildly. If ν_2 is excluded, ν_4 has a minimum at 90° and a maximum at 120° while ν_1 becomes a horizontal zigzag. In either case, ν_3 remains flat. Some of the results of the decomposition have been combined in figure 8.

The decomposition at 8 eV constitutes the first experimental observation of the distinct angular distributions of ν_1 and ν_3. A similar pattern, albeit more symmetrical

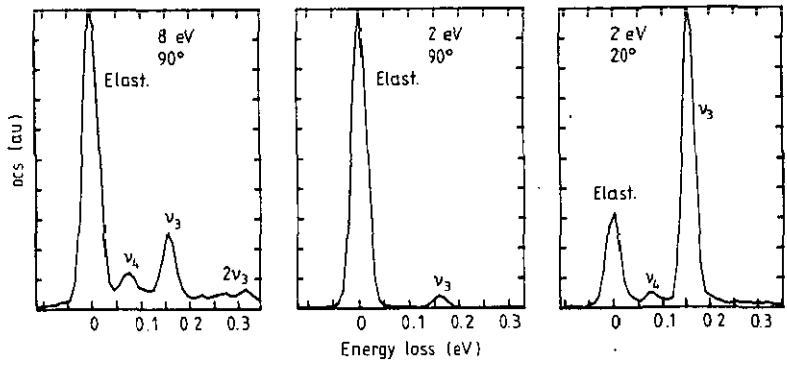

Figure 6. Electron energy loss spectra for vibrational excitation.

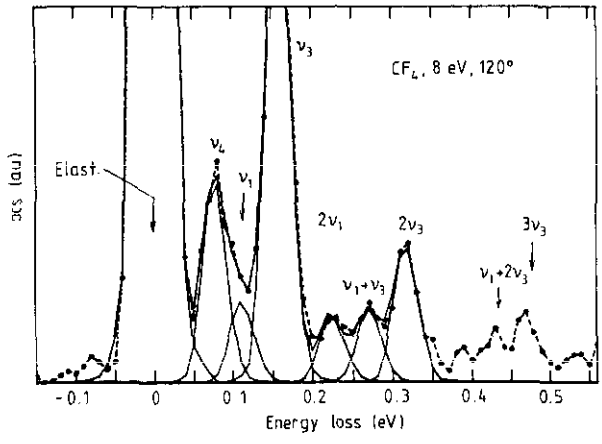

Figure 7. Example of decomposition up to and including $2\nu_3$. The back ground has been subtracted out. At the left a small superelastic peak can be seen (nozzle is heated).

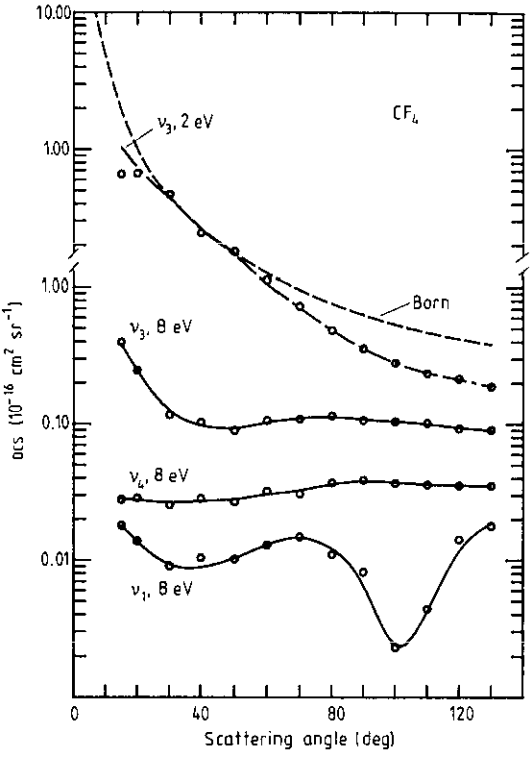

Figure 8. Decomposed vibrational mode ν_3 for an impact energy of 2 eV (— —) together with the Born dipole approximation. Decomposed vibrational modes ν_1, ν_3, and ν_4 for 8 eV impact energy (——). The signal-to-noise ratio deteriorates for decreasing DCS.

around 90°, was previously obtained from a CMS calculation for SiH_4 (Tanaka *et al* 1990a) and in a somewhat ambitious fit (10 parameters with 12 data points) of angular correlation theory (Tanaka *et al* 1983) for CH_4.

For excitation near threshold (2 eV) only ν_3 could be clearly observed over the whole angular range (ν_4 appears only at 15° and 20° with a size of approximately $\frac{1}{10}$ of ν_3). No harmonics of ν_3 were found.

4. Symmetry analysis

4.1. Preliminaries

In general, the broad hump in the total cross sections is connected with a shape resonance as previously discussed for CH_4 (Boesten and Tanaka 1991b), Si_2H_6 (Tanaka *et al* 1988), C_2H_6 (Boesten *et al* 1990), SiH_4 (Tanaka *et al* 1990a) and GeH_4 (Tanaka *et al* 1990b). We assume that the shape resonance reflects the existence of a compound state consisting of a molecule in the ground state plus an electron temporarily trapped in a low-lying unoccupied orbital. The ground-state configuration of CF_4

$$\ldots(4a_1)^2(3t_2)^6(1e)^4(4t_2)^6(1t_1)^6\ {}^1A_1$$

belongs to the T_d point group. In addition to the two lowest unoccupied orbitals belonging to the a_1 and t_2 irreducible representations (Tossel and Davenport 1984) we

consider the orbital of species e which was included in the analysis by Huo. Since the ground state belongs to the A_1 representation these orbitals determine the symmetry species of the corresponding compound state. The transition operator H between the initial and final states ψ_i and ψ_f has the same symmetry as the charge density of the compound state (Wong *et al* 1975) and this is given by its symmetric product: (1) $A_1 \times A_1 = A_1$, (2) $(T_2 \times T_2)_s = A_1, E, T_2$ and (3) $(E \times E)_s = A_1, E$. The direct product rules for $\langle \psi_i | H | \psi_f \rangle \neq 0$ then allow one to calculate the symmetry species of the final state as A_1 (1), A_1, E, T_2 (2) and E (3). Γ_e of the outgoing e-wave can be obtained from $\psi_f \times \Gamma_e = \Gamma_r$ where r indicates the resonant state (Andrick and Read 1971). These calculations are summarized in table 2 which also includes the l-values for an expansion of the outgoing wave in spherical harmonics that belong to Γ_e (Altman 1957, Altmann and Bradley 1962). Here, l refers to a molecule-fixed frame. Resonant state A_2 was excluded because of its large centrifugal barrier, $l \geqslant 6$.

Table 2. Symmetry species.

ψ_i	Resonant state	ψ_f	Vibrational mode	Outgoing e-wave	Allowed l†
A_1	T_2	A_1	$\nu_{1,0}$	t_2	1, 2, 3, 4
A_1	T_2	E	ν_2	t_1	3, 4, 5, 6
				t_2	1, 2, 3, 4
A_1	T_2	T_2	$\nu_{3,4}$	a_1	0, 3, 4, 6
				e	2, 4, 5, 6
				t_1	3, 4, 5, 6
				t_2	1, 2, 3, 4
A_1	E	A_1	$\nu_{1,0}$	e	2, 4, 5, 6
		E	ν_2	e	2, 4, 5, 6
A_1	A_1	A_1	$\nu_{1,0}$	a_1	0, 3, 4, 6

† Of the outgoing wave in a molecular fixed system. Allowed l for A_2: 6, 9, 10, 12. ν_0 = elastic scattering.

According to the theory of angular correlations (Read 1968, Andrick and Read 1971), the angular distribution function $W(k_i, k_f)$ for purely resonant scattering of electrons from molecules in a rotationally stationary approximation with the molecule left in a final vibrational mode, can be expressed as

$$W(k_i, k_f) = \sum_k A_k P_k(\cos\theta) \tag{4}$$

with A_k given by a complicated formula (equation (8) of Andrick and Read) which we simplify for the present purposes as:

$$A_k = \sum \sum_q A_q \begin{pmatrix} l_1 & l_1' & k \\ 0 & 0 & 0 \end{pmatrix} \begin{pmatrix} l_2 & l_2' & k \\ 0 & 0 & 0 \end{pmatrix} \tag{5}$$

where the first sum is over $l_1 l_1' l_2 l_2'$ and q combines all other summing indices of Andrick's formula. The braces are Clebsch-Gordan coefficients and l_1, l_2 refer to the incoming and outgoing waves in the molecule-fixed frame. Note that the derivation of $W(k_i, k_f)$

assumes isolated (non-coupled) resonant states. The Clebsch-Gordan coefficients arise from the product of four rotational matrices averaged over the orientations of the target molecule and thus appear in formulae for elastic scattering, vibrational excitation, and rotational excitation (cf Gianturco and Jain 1986, section 6). The well known conditions on the Clebsch-Gordan coefficients $l+l'-k \geq 0$, $l-l'+k \geq 0$ and $l'-l+k \geq 0$ restrict the allowed values of l.

We now assume that a human inspector can approximately locate the maxima and minima in the angular distributions of the observed DCS even if they ride on a background of direct scattering, and thus identify the low-order Legendre polynomials P_k needed to describe the angular behaviour†. It may require a comparison of the wave shapes at energies above and below a suspected resonance, cf table 3 which also includes some vibrational observations.

Table 3. Position of observed maxima and minima in deg. k refers to the Legendre polynomials P_k of approximately similar shape; two k values indicate a sum $P_{k1}+P_{k2}$.

eV		Min.	Max.	Min.	Max.	Min.	Required k
5	elast.	20	55	120	—	—	
8†	elast.	30	55	90	115	—	2+6
15	elast.	30	40	60	90	120	
10	elast.	25	35?	70	95	120	
20†	elast.	55	80	110	—	—	4
50	elast.	35	50	90	—	—	
8	ν_1	35	70	105	130	—	5
	$\nu_{3,4}$	—	—	—	—	—	0
20	ν_3	—	—	—	—	—	0
	ν_2	50?	90?	—	—	—	4
	ν_4	90?	120?	—	—	—	4

† Centre of assumed shape resonance.

4.2. Partial wave interference and coupled resonances?

Following an initially experimental observation in resonances of C_6H_6 (Wong and Schulz 1975), Gallup (1986) has demonstrated with an approximate R-matrix method that the principal partial wave of a resonance can interfere with a non-resonant s-wave to produce a different set of vibrations. However, in a highly symmetric molecule such as CF_4, decay of a T_2 resonant state already can excite all vibrational fundamental modes, so that it would be difficult to distinguish the excitation processes experimentally. Also note that we did not observe any isotropic ν_1 mode.

Similarly, Estrada *et al* (1986) studied the possibility of vibronic coupling of two or more close-lying resonances through nuclear motion, and attribute the intense excitation of single quanta of non-totally symmetric modes to such a coupling. If scattering in the isolated states is dominated by a single l, a strong dependence of the

† In experimental jargon, and referring immediately to P_l^2 which has the same number of peaks as P_{2l}, one simply identifies the angular distribution as 'p waves', 'f waves' etc.

angular factors of the DCS on energy and an asymmetric shape of the DCS are indications for the presence of coupled resonances. From a model calculation they conclude that in a 'competition' between a wide and a narrow resonance the narrow peak widens, and that coupling between resonances provides an efficient mechanism for the excitation of odd quanta of non-totally symmetric vibrations. Furthermore, 'vibronic coupling can markedly influence ... the behaviour of the vibrational excitation cross sections at threshold'. Some of these trends seem to be present in our vibrational observations. The only candidates for a vibrational coupling would be $\nu_{3,4}$ connecting resonant states T_2 and E, or the optically forbidden ν_2 coupling state A_1 with E or T_2. This can easily be shown from the direct product rule $\Gamma_1 \times \Gamma_u \times \Gamma_2 \supset \Gamma_{tot.sym}$ for $\Gamma_1 \neq \Gamma_2$ and a non-totally vibrational mode u (Estrada *et al*, equation (10)). Unfortunately, their paper is restricted to Abelian point groups and thus excludes the symmetry T_d of CF_4.

4.3. 8 eV shape resonance

A quick inspection of the three-dimensional DCS in figure 1 reveals a local bump at around 8 eV, 50°, also see table 3. Its angular distribution requires Legendre polynomials of order $k = 2$ and $k = 6$. If the bump is due to a shape resonance, the Clebsch-Gordan coefficients lead to $l = l' = 1$ (or $l = 0$, $l' = 2$) for $k = 2$, and to $l = l' = 3$ (or $l = 2$, $l' = 4$) for $k = 6$. The vibrational excitation of ν_1 requires $k = 5$, or $l + l' \geq 5$, i.e. $l = l' = 3$ (or $l = 1$, $l' = 4$ or $l = 2$, $l' = 3$). Similarly, the flat behaviour of $\nu_{3,4}$ leads to $k = 0$ and $l = 0$. The only resonance fulfilling these conditions is T_2, cf table 2. Huo calculated a resonance at around 6.6 eV of symmetry T_2 with $l = 1$.

4.4. 20–21 eV shape resonance

A small local bump appears at around 20 eV, 80° in the three-dimensional plot, and seems to be confirmed as such in table 2. Its shape requires $k = 4$, and consequently $l = l' = 2$ (or $l = 1$, $l' = 3$) while again, ν_3 is flat with $l = 0$. The ambiguous results for ν_2 and ν_4 would require $k = 4$ and $k = 6$ (the latter with $l = l' = 3$ or $l = 2$, $l' = 4$). Again only a resonance of species T_2 can fulfill these requirements. Huo's second T_2 resonance is centred at 23 eV (from her figure 3) and was attributed to an $l = 2$ partial wave. We could not detect any independent resonance of species E at around 28 eV in the elastic DCS as calculated by Huo. Similarly, from the lack of structure in figure 5, it seems unlikely that the two broad resonant states (T_2 at 21 eV and E at 28 eV, Huo) would be coupled by a ν_3 vibrational mode as to be expected from the analysis by Estrada *et al* (1986).

4.5. Threshold peak at 2 → 0.8 eV

We now refer to the steep ascent at the left of figure 5, also see figure 6. It is likely that our excitation measurements have not yet reached their peak since swarm experiments (Kurachi and Nakamura 1990) report integrated cross section of ν_3 which steadily increase towards a maximum of 1.3×10^{-15} cm^2 at about 0.2 eV.

(i) In modes with a large IR activity, direct dipole scattering will produce large cross sections near threshold. Thus the strongly forward peaked angular distribution of ν_3 (figure 8, 2 eV) most likely indicates direct scattering. It coincides approximately with the Born dipole-approximation (Itikawa 1974, DCS $(0°) = 73 \times 10^{-16}$ cm^2 sr^{-1}) if one neglects the experimentally difficult low angle measurement at 15°, see figure 8. Here we have used an IR intensity of $\Gamma_3 = 80$ cm^2 mmol^{-1} (Koschel *et al* 1974, averaged);

the IR intensity of Bishop and Cheung (1982) would produce 10% smaller Born cross sections. A further confirmation of direct scattering arises from the absence of harmonics in accordance with the selection rule $\Delta v = \pm 1$ (Davis *et al* 1972). The disagreement at larger angles $>60°$ may be due to limiations of the Born approximation which results from only the first term of the power series $(1/\Delta k^4)(a\Delta k^2 + b\Delta k^4 + \ldots)$, cf Itikawa (1974).

A similar strongly forwarded peak was observed for SF_6 (Rohr 1977), attributed to dipole interaction and clearly distinguished from threshold effects which usually show a flat angular distribution (for polar molecules see Rohr *et al* 1978, Herzenberg 1984, sections 2 and 3; for CH_4 see Sohn *et al* 1983). Relatively strong scattering due to a large transition dipole moment has also been found in preliminary investigations on C_2F_6 in this laboratory.

The large transition dipole moment (absent in CH_4) must be connected with the fluorine. In the CMS calculations of Tossel and Davenport (1984) on CX_4 and SiX_4 molecules, large elastic cross sections near threshold arise for X = F and X = Cl, but not for X = H; they are attributed to component a_1 and are sensitive to variations in polarizability. Both F and Cl have large electron affinities. Similarly a CMS calculation (Dehmer *et al* 1978) on $e^- + SF_6$ scattering assigns the large peak at thermal energies to component a_{1g}. Unfortunately, Huo's calculations exclude the lower energy region below 5 eV (polarization not included).

(ii) The measurements show a slight shoulder at 40–50°. If this indicates an underlying shape resonance, mode ν_3 excitation requires a T_2 resonant state (cf table 2, also see Curtis and Walker (1989)). Whether direct scattering also hides a true vibrational threshold peak cannot be decided from our data alone. If so one would expect a rather flat angular distribution.

A low-lying TNI resonance has been reported previously. Verhaart *et al* (1978) observed a short progression of frequency ν_3 in a transmission experiment on CF_4^- and assigned the extra electron to a Rydberg type orbital because the spacings so closely match those of a neutral molecule. Curtis and Walker (1989) found six steps in a signal from a trapped-electron spectrometer; furthermore, the first dip of this progression can also be recognized in the integral total cross sections of Field *et al* (1984). Robin (1985) denies the existence of such non-bonding 3s orbitals in anions. He points out that fluorination drastically lowers σ MO including σ^* and assigns the configuration of the 0.5 eV valence TNI resonance as $^2(N, a_1\sigma^*)$. The progression is interpreted as an excitation of vibrational mode ν_3'. Note that if the resonant state is of symmetry A_1 the resonance must be either a Feshbach resonance or some other trapping mechanism but cannot be a shape resonance.

(iii) One such trapping mechanism has been proposed in the context of very slow electron attachment to SF_6 ($Q_a > 2 \times 10^{-14}$ cm^2, Chutjian 1981). Gauyacq and Herzenberg (1984) describe a non-adiabatic model which assumes a large molecule close to the birth of a new bound state with a large s-component. They show that the molecule can slip into this state by a small displacement of the nuclear framework. For SF_6 the state is stable, for CF_4 however, the electron affinity is negative −0.7 eV (Christodoulides *et al* 1984).

From these considerations the enhancement near threshold must be attributed to the optically allowed transition. There may be a simultaneous resonance, details of which cannot be determined from the present measurements. The enhancement at 8 eV follows standard patterns of shape resonances, with at least three harmonics of ν_3 clearly visible. The signal at 20 eV is too weak to observe harmonics.

Acknowledgment

We want to thank Dr M Inokuti of ANL for helpful discussions.

References

Altmann S L 1957 *Proc. Camb. Phil. Soc.* **53** 343-67
Altmann S L and Bradley C J 1962 *Phil. Trans. R. Soc.* A **255** 199-215
Andrick D and Read F H 1971 *J. Phys. B: At. Mol. Phys.* **4** 389-96
Bishop D M and Cheung L M 1982 *J. Phys. Chem. Ref. Data* **11** 119-33
Boesten L and Tanaka H 1991a *At. Data* to be submitted
—— 1991b *J. Phys. B: At. Mol. Opt. Phys.* **24** 821-32
Boesten L, Tanaka H, Sato H, Kimura M, Dillon M A and Spence D 1990 *J. Phys. B: At. Mol. Opt. Phys.* **23** 1905-13
Chutjian A 1981 *Phys. Rev. Lett.* **46** 1511-4
Christodoulides A A, McCorkle D L and Christophorou L G 1984 *Electron-Molecule Interactions and their Applications* vol II ed L G Christophorou (New York: Academic) p 549
Christophorou L G 1984 *Electron-Molecule Interactions and their Applications* vol II (New York: Academic) pp 393-6
Curtis M G and Walker I C 1989 *J. Chem. Soc. Faraday Trans.* **2** 659-70
Curtis M G, Walker I C and Mathieson K J 1988 *J. Phys. D: Appl. Phys.* **21** 1271-4
Davis H T and Schmidt L D 1972 *Chem. Phys. Lett.* **16** 260-4
Dehmer J L, Siegel J and Dill D 1978 *J. Chem. Phys.* **69** 5205-6
Estrada H, Cederbaum L S and Domcke W 1986 *J. Chem. Phys.* **84** 152-69
Field D, Ziesel J P, Guyon P M and Govers T R 1984 *J. Phys. B: At. Mol. Phys.* **17** 4565-75
Gallup G A 1986 *Phys. Rev.* A **34** 2746-50
Gauyacq J P and Herzenberg A 1984 *J. Phys. B: At. Mol. Phys.* **17** 1155-71
Gianturco F A and Jain A 1986 *Phys. Rep.* **143** 347-425
Harland P W and Franklin J L 1974 *J. Chem. Phys.* **61** 1621-36
Harshbarger W R and Lassettre E N 1973 *J. Chem. Phys.* **58** 1505-13
Hayashi M 1987 *Swarm Studies and Inelastic Electron-Molecule Collisions* ed L C Pitchford, B V McKoy, A Chutjian and S Trajmar (New York: Springer) pp 167-87
—— 1991 Private communication
Herzenberg A 1984 *Electron Molecule Collisions* ed I Shimamura and K Takayanagi (New York: Plenum) pp 191-274
Huo W M 1988 *Phys. Rev.* A **38** 3303-9
Itikawa Y 1974 *J. Phys. Soc. Japan* **36** 1127-32
Jones R K 1986 *J. Chem. Phys.* **84** 813-9
King G C and McConkey J W 1978 *J. Phys. B: At. Mol. Phys.* **11** 1861-77
Koschel D, Kirschstein G and Ruprecht S 1974 *Gmelin's Handb. Anorg. Chemie, C-D2* (Berlin: Springer) p 129
Kurachi M and Nakamura H 1990 *Proc. 13th. Symp. on Ion Sources and Ion-Assisted Techn. (Tokyo)* ed T Takagi (Kyoto: Kyoto University) pp 205-8
Leiter K, Deutsch H and Märk T D 1984 *Symp. on Atomic and Surface Physics* ed F Howorka *et al* (Innsbruck: University of Innsbruck) pp 39-44
Lotter J, Kühn A and Illenberger E 1989 *Chem. Phys. Lett.* **157** 171-4
MacNeil K A G and Thynne J C J 1970 *Int. J. Mass Spectrom., Ion Phys.* **3** 445-64
Naidu M S and Prasad A N 1972 *J. Phys. D: Appl. Phys.* **5** 983-93
Nishimura H 1991 Private communication
Read F H 1968 *J. Phys. B: At. Mol. Phys.* **2** 893-908
Robin M 1985 *Higher Excited States of Polyatomic Molecules* vol 3 (New York: Academic) p 125
Rohr K 1977 *J. Phys. B: At. Mol. Phys.* **10** 1175-9
—— 1978 *J. Phys. B: At. Mol. Phys.* **11** 4109-17
Scheunemann H U, Heni M, Illenberger E and Baumgärtel H 1982 *Ber. Bunsenges. Phys. Chem.* **86** 321-6
Sakae T, Sumiyoshi S, Murakami E, Matsumoto Y, Ishibashi K and Katase A 1989 *J. Phys. B: At. Mol. Opt. Phys.* **22** 1385-94
Sohn W, Jung K and Ehrhardt H 1983 *J. Phys. B: At. Mol. Phys.* **16** 891-901
Spyrou S M, Sauers I and Christophorou L G 1983 *J. Chem. Phys.* **78** 7200-16

Tanaka H, Boesten L, Matsunaga D and Kudo T 1988 *J. Phys. B: At. Mol. Opt. Phys.* **21** 1255–63
Tanaka H, Boesten L, Sato H, Dillon M A and Kimura M 1990b *43rd GEC 16–19* (American Physical Society) Abstracts
Tanaka H, Boesten L, Sato H, Kimura M, Dillon M A and Spence D 1990a *J. Phys. B: At. Mol. Opt. Phys.* **23** 577–88
Tanaka H, Kubo M, Onodera N and Suzuki A 1983 *J. Phys. B: At. Mol. Phys.* **16** 2861–9
Tossel J A and Davenport J W 1984 *J. Chem. Phys.* **80** 813–21
Verhaart G J, Van der Hart W J and Brongersma H H 1978 *J. Chem. Phys.* **34** 161–9
Wong S F and Schulz G J 1975 *Phys. Rev. Lett.* **35** 1429–32
Winters H F and Inokuti M 1982 *Phys. Rev.* A **25** 1420–30